

Distribution and height of methane bubble plumes on the Cascadia Margin characterized by acoustic imaging

Katja U. Heeschen

Research Center for Marine Geosciences, Research Center for Marine Geology, Kiel, Germany

Anne M. Tréhu and Robert W. Collier

College of Oceanographic and Atmospheric Sciences, Oregon State University, Corvallis, Oregon, USA

Erwin Suess and Gregor Rehder

Research Center for Marine Geosciences, Research Center for Marine Geology, Kiel, Germany

Received 23 January 2003; accepted 26 March 2003; published XX Month 2003.

[1] Submersible investigations of the Cascadia accretionary complex have identified localized venting of methane gas bubbles in association with gas hydrate occurrence. Acoustic profiles of these bubble plumes in the water column in the vicinity of Hydrate Ridge offshore Oregon provide new constraints on the spatial distribution of these gas vents and the fate of the gas in the water column. The gas vent sites remained active over the span of two years, but varied dramatically on time scales of a few hours. All plumes emanated from local topographic highs near the summit of ridge structures. The acoustic images of the bubble plumes in the water column disappear at water depths between 500 to 460 m, independent of the seafloor depth. This coincides with the predicted depth of the gas hydrate stability boundary of 510 to 490 m, suggesting that the presence of a hydrate skin on the bubble surface prevents them from rapid dissolution. The upper limit of the acoustic bubble plumes at 460 m suggests that dissolution of the residual bubbles is relatively rapid above the hydrate stability zone. **INDEX TERMS:** 4820 Oceanography: Biological and Chemical: Gases; 4259 Oceanography: General: Ocean acoustics; 4806 Oceanography: Biological and Chemical: Carbon cycling. **Citation:** Heeschen, K. U., A. M. Tréhu, R. W. Collier, E. Suess, and G. Rehder, Distribution and height of methane bubble plumes on the Cascadia Margin characterized by acoustic imaging, *Geophys. Res. Lett.*, 30(0), XXXX, doi:10.1029/2003GL016974, 2003.

1. Introduction

[2] Recently a number of gas bubble plumes, containing mostly methane (CH₄) gas, have been discovered by acoustic methods to rise over the slopes of continental margins, apparently in association with the formation of gas hydrates; e.g., in the Guayamas Basin [Merewether *et al.*, 1985], in the Gulf of Mexico [MacDonald *et al.*, 2002], at Blake Ridge [Paull *et al.*, 1995], on the Sakhalin slope in the Sea of Okhotsk [Salyuk *et al.*, 2002] and along the Cascadia accretionary complex [Suess *et al.*, 2001]. These gas bubble plumes originate at sites as deep as 2500 m, and they have been observed to rise as much as 900 m in the water column [Merewether *et al.*, 1985]. Along the Sakhalin slope (above

1000 m depth), acoustic signals often seem to vanish between 300 to 500 m depth below the sea surface [Biebow *et al.*, 2000]. Often, however, the minimum depth in the water column at which the gas bubbles disappear is poorly resolved and in some cases the plumes extend to the sea surface. Furthermore, the persistence of these CH₄ gas bubble plumes in the ocean is remarkable because the ocean is undersaturated in methane, and the bubbles should quickly dissolve. Based on an observed correlation between bubble size and rise rate, Merewether *et al.* [1985] inferred that the CH₄ bubbles were protected by a coating of oil or gas hydrate. The latter was suggested to cause the reduced shrinking rate of methane gas bubbles, which was observed in a CH₄ gas release experiment carried out in the gas hydrate stability zone (GHSZ) in the ocean [Rehder *et al.*, 2002]. The gas hydrate coating should dissociate when the bubbles exit the GHSZ. A coating of oil, on the other hand should sufficiently protect the bubbles from dissolution until they reach the sea surface, as indicated in the Gulf of Mexico [MacDonald *et al.*, 2002].

[3] In this paper, we use the acoustic backscatter from bubbles in the water column to determine the spatial distribution of bubble plumes and develop a hypothesis about their relation to the water depth along the middle and lower slope of the central Oregon continental margin.

2. Geologic Setting

[4] At the Cascadia subduction zone, the Juan de Fuca Plate is subducting obliquely beneath the continental North American plate. A large accretionary wedge has developed, characterized by a series of discontinuous topographic highs, offshore from central Oregon [MacKay *et al.*, 1992] (Figure 1). A strong bottom-simulating reflection (BSR) is widespread at water depths between approximately 600 and 1500 m [Tréhu *et al.*, 1999], indicating the presence of free gas underlying a region in which gas hydrate is stable. The BSR is particularly strong beneath topographic highs such as North Hydrate Ridge (NHR), South Hydrate Ridge (SHR), Southeast Knoll (SEK) and Northwest Knoll (NWK). On NHR, the presence of sub-seafloor gas hydrates was confirmed during ODP Leg 146 [Carson *et al.*, 1995]. At SHR gas hydrates were found at the seafloor [Suess *et al.*, 1999]. Free gas, containing 99% CH₄ [Torres *et al.*, 2002], and methane-rich fluids are channeled upwards

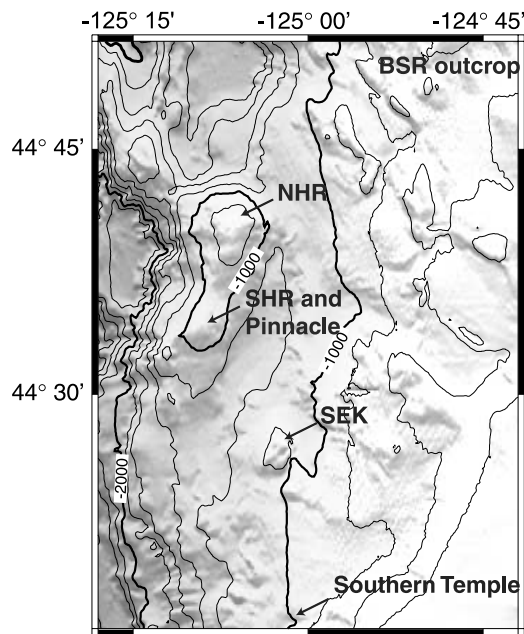


Figure 1. Bathymetry of the study area and sites of acoustic surveys. NHR = Northern Hydrate Ridge, SEK = Southeast Knoll, SHR = Southern Hydrate Ridge.

95 through faults to feed vents at the seafloor [e.g., Carson *et al.*, 1995; Suess *et al.*, 1999, 2001; Torres *et al.*, 2002].

96 [5] During the TECFLUX (TECtonically-induced material FLUXes) program, a wide variety of video-guided tools
 97 (e.g., OFOS, TV-MUC, benthic landers), water and gas
 98 samplers, and submersibles were used to investigate venting
 99 processes at the Oregon continental margin [Linke *et al.*,
 100 2001; Suess *et al.*, 2001; Torres *et al.*, 2002]. Active
 101 methane gas ebullition was observed at NHR, SHR, and
 102 SEK. Echosounding systems using 12.5 and 18 kHz proved
 103 to be of great use for imaging these bubble plumes in the
 104 water column, and aided in locating and sampling of vent
 105 sites. Suess *et al.* [2001] describe the detection of an
 106 acoustic anomaly extending more than 200 m above SHR
 107 and the simultaneous observation of vigorous bubbling at
 108 the seafloor.
 109
 110

111 3. Methods

112 [6] Acoustic detection is a particularly suitable tool for
 113 finding and characterizing gas bubbles in the ocean. It is

114 based on the strong absorption and scattering effects of
 115 sound by gas bubbles, which are enhanced by a factor of
 116 $10^3 - 10^4$ at the particular resonance frequency of the bubble.
 117 According to Clay and Medwin [1977], the bubble resonant
 118 frequency is inversely proportional to the bubble radius. It
 119 also depends on the water depth such that the bubble
 120 resonant radii increase with depth. Compared to a rigid
 121 phase of the same size, the acoustic effects of a resonant
 122 bubble are greater by $10^{10} - 10^{11}$ [Clay and Medwin, 1977].

123 [7] Backscattered sound was used to detect gas bubbles
 124 in the water column during five cruises in 1999 and 2000,
 125 including detailed surveys at NHR, SHR, and SEK (Table 1).
 126 On all acoustic surveys carried out for mapping of bubble
 127 plumes we used a source with a frequency of 12.5 kHz and
 128 a beam width of 15° , resulting in a swath width of roughly
 129 160 m at 600 m water depth and 210 m at 800 m depth. The
 130 swath width of the acoustic beam on a moving ship leads to
 131 a distortion of the actual width of the bubble plumes. The
 132 widths of the acoustic signals therefore overestimate the
 133 width of the bubble plumes in the water column by about as
 134 much as the swath width. The 18 kHz acoustic system of
 135 SONNE with a beam width of 20° was used for guidance of
 136 water column sampling only and the results are not inte-
 137 grated into the acoustic surveys (Table 1). However, the
 138 upper limits of the acoustic plumes equal those of the 12.5
 139 kHz signals within the given resolution. The bubble resonant
 140 radii at the given source frequencies and water depths were
 141 2.3 mm (700 m) and 2.0 mm (500 m) for the 12.5 kHz source
 142 and 1.6 mm (700 m) and 1.3 mm (500 m) for 18 kHz,
 143 respectively ($Ka \gg 1$ [Clay and Medwin, 1977, equation
 144 6.3.10]). While acoustic plumes were detected with the 12.5
 145 and 18 kHz sources and showed equivalent distributions, a
 146 3.5 kHz source simultaneously used with a few 12.5 kHz
 147 observations did not detect acoustic plumes. It can be
 148 assumed that bubbles with the corresponding resonant radii
 149 of 6.6 to 7.8 mm were absent. These observations are in
 150 agreement with video analysis from and Rehder *et al.* [2002],
 151 who observed average bubble radii of 2.5 to 4 mm at the gas
 152 vents of SHR immediately after leaving the seafloor. From
 153 video observations the opening of the conduits where the
 154 bubbles pass through were estimated to have radii of 2 to 5.5
 155 mm at NHR, which about equals the size of the bubbles and
 156 is comparable to the vent at SHR [Torres *et al.*, 2002].

157 [8] The acoustic systems available on the ships were not
 158 specialized for the detection of bubbles in the water column
 159 and it was not possible to post-process digital records of the
 160 data. Thus it is likely that we were not able to detect few
 161 single bubbles with radii different from the resonant radius,

t1.1 **Table 1.** List of Cruises Including Acoustic Surveys and Acoustic Guidance During Hydrocast Stations

t1.2	Cruise	RV	Dates	System used	Acoustic Survey
t1.3	AT3-35B [Torres <i>et al.</i> , 1999]	Atlantis	30 Jun–13 Jul 1999	SEABeam 2000 3.5/12.5 kHz (12.5 kHz)	NHR-I, II, II SEK-I, II Southern Temple BSR-Outcrop SHR-vent site, Pinnacle
t1.4	SO143 [Bohrmann <i>et al.</i> , 1999]	Sonne	31 Jul–25 Aug 1999	STN Atlas Elektronik 4/18 kHz (18 kHz)	hydrocast series at SHR
t1.5	W1099a	Wecoma	01 Oct–05 Oct 1999	Knudsen 320BR 3.5/12.5 kHz (12.5 kHz)	hydrocasts at NHR NHR-IV
t1.6	SO148 [Linke <i>et al.</i> , 2001]	Sonne	20 Jul–15 Aug 2000	STN Atlas Elektronik 4/18 kHz (18 kHz)	hydrocasts at SEK
t1.7	TN112 [Tréhu and Bangs, 2001]	Thompson	19 June–3 July 2000	SEABeam 2000 3.5/12.5 kHz (12.5 kHz)	SHR-I SEK
t1.8	Eastern daylight time (EDT).				

162 which should be found at the very top of disperse bubble
163 plumes.

164 4. Observations and Discussion

165 [9] Strong acoustic signatures indicative of bubble
166 plumes in the ocean were observed near the summits of
167 NHR, SEK and SHR (Figure 2a–2c). They were found in
168 surveys conducted 1 to 2 years apart, suggesting that they
169 are robust features with a lifetime of at least a few years. In
170 contrast, no acoustic plumes were found at other potential
171 sites, such as: ‘Southern Temple’, an unusual topographic
172 feature that resembles a mud volcano; the ‘BSR-Outcrop’, a
173 site where a strong BSR intersects the seafloor [Tréhu *et al.*,
174 1995]; the ‘Pinnacle chemoherm’, a 30 m high carbonate
175 pinnacle 250 m southwest of the summit of SHR (see Figure 1
176 for locations).

177 [10] The acoustic plumes at NHR and SEK overlie local
178 topographic highs which correspond to regions of very high
179 seafloor reflectivity in side scan sonar observations [Clague
180 *et al.*, 2001]. Seafloor video indicates that these include
181 ‘chemoherms’, massive structures formed from authigenic
182 carbonates [Greinert *et al.*, 2001; Linke *et al.*, 2001]. The
183 acoustic plume at SHR is also found at a topographic high,
184 but here the seafloor reflectivity is intermediate in strength,
185 corresponding to a region where massive hydrate is abun-
186 dant in the shallow subsurface [Suess *et al.*, 2001].

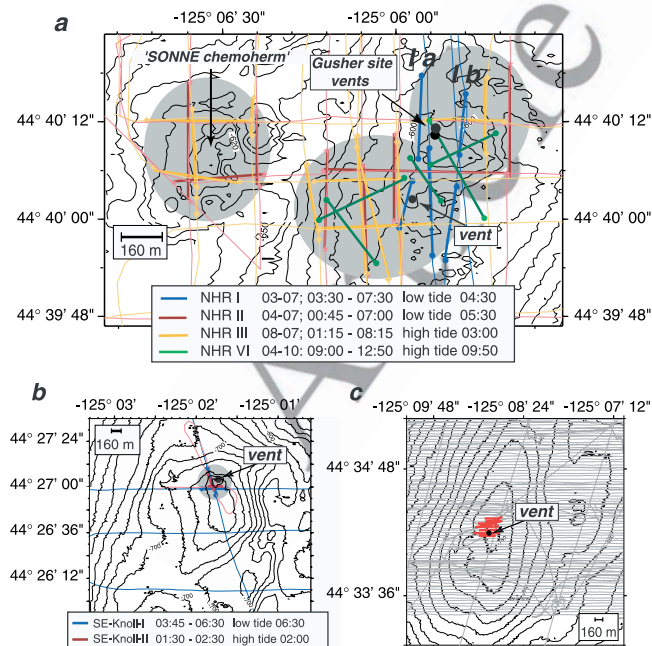


Figure 2. Detailed acoustic surveys completed at NHR, SEK, SHR; (a) Four repeated surveys (thin lines) at NHR show three distinct locations with acoustic signals (gray shaded areas). The thick colored lines represent the location of the acoustic signals during the various surveys. I a and I b mark the survey lines shown in Figure 3. (b) At SEK two surveys were completed which found one acoustic signal. (c) One acoustic signal was found at SHR. The black dots indicate the locations at which gas vents were seen with submersibles and ROPOS [Torres *et al.*, 1999; Linke *et al.*, 2001; Tryon *et al.*, 2002].

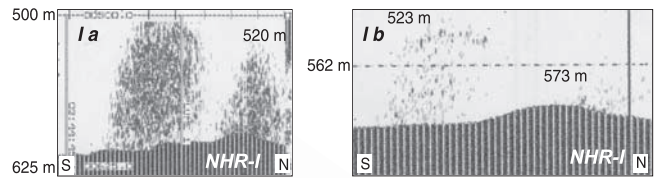


Figure 3. Examples of the variable strength and width of acoustic plumes at NHR from crossings I a and I b of survey NHR-I. The locations are shown in Figure 2. The depths indicated above the acoustic signals mark the upper limits of the detected backscatter. The x-axis is not in scale.

[11] Whereas SHR and SEK each had one distinct plume, three separate bubble plumes were observed simultaneously in the water column above NHR (Figure 2). At SEK and SHR, the vent sites found with submersibles coincide with the acoustic signals in the water column, while at NHR, submersible observations are only available for two of the three acoustic plumes (Figure 2). The vent site at the so-called ‘SONNE chemoherm’ of NHR has not yet been subject to video observation. However, the gas venting in this location is strongly suggested by the repeated occurrence of an acoustic signal and also indicated by methane enrichments in hydrocast samples of cruise SO143 [Bohrmann *et al.*, 1999]. The discovery in acoustic signals of three gas vent areas at NHR implies that the methane gas flux calculated from submersible observations of the Gusher site vents alone by Torres *et al.* [2002] is probably underestimated. They calculated a gas flux of $6 \cdot 10^4 \text{ mol day}^{-1}$ for NHR. Long-term acoustic observations with calibrated, digital instruments are needed to obtain a precise estimate of the gas fluxes from unequally distributed vent areas.

[12] Despite the limitation of our acoustic observations, the data still provide insights into temporal variability and persistence of the plumes over the two years of investigations. Whereas the plume positions were rather stable and the plumes remained active over the time-scale of the investigation, the strength and width of the acoustic signals were highly variable over a time-scale of a few hours. This is demonstrated in Figures 2 and 3. The width of the acoustic plumes varied between 100 and 600 m. Taking into account the swath width of the acoustic beam of 130 to 210 m at 500 to 800 m water depth, this corresponds to variations between thin bubble streams and bubble plumes of several 100 m in diameter. In addition, the plumes even vanished on a few occasions. Unlike surveys NHR-I and NHR-III, no acoustic bubble plume was detected at the same position (line 1) of survey NHR II (Figure 2a). Similar variability was seen elsewhere at SEK (Figure 2b), at SHR (Figure 2c) and on a long-term observation on cruise SO148, where an acoustic plume, which was recorded steadily for 1.5 hours at SHR, completely vanished within minutes. A feature also observed by video at the gas vents [Torres *et al.*, 1999].

[13] These variations may reasonably be explained by temporal changes in the gas venting rates. At the Gusher vent site at NHR, video guided observations of a single vent site showed a good correlation between a weakening or even absence of gas venting and high tide, whereas hydrocast investigations at SHR did not indicate this behavior [Torres *et al.*, 2002; K. Nakamura, Geological Survey of

236 Japan, personal communication, 2002; *Heeschen and Col-*
 237 *lier*, 2002]. The acoustic bubble detection frequently pre-
 238 sented strong plumes during high tide at both summits,
 239 NHR and SHR (44°40'12'N; surveys NHR-II and NHR-III;
 240 Figure 2a). These observations suggest that diverse mech-
 241 anisms control the gas release, which is only partly related
 242 to changes caused by the tidal cycle as also suggested by
 243 *Tryon et al.* [1999, 2002].

244 [14] On all surveys the tops of the acoustic plumes, were
 245 observed at heights of 540–470 m below the sea surface at
 246 all gas vent sites, even though the seafloor depth ranged
 247 from 590 m at NHR to 780 m at SHR (Figure 4). Strong
 248 signals from the center of the well-mapped plumes generally
 249 rose to a depth of 480 ± 20 m. Weaker signals extended
 250 between 540 to 500 m below the sea surface, which might
 251 in part be due to the sideswipes of the gas plumes. These
 252 acoustic observations of the height of bubble plumes in the
 253 water column are supported by submersible monitoring of
 254 the rising gas bubbles conducted within the plumes at NHR.
 255 In the field of view of the submersible a clear decrease in
 256 the number and size of bubbles was observed at about 450 m
 257 depth [*Linke et al.*, 2001; *Suess et al.*, 2001].

258 [15] Usually the dissolution rate of rising gas bubbles is
 259 controlled by the partial pressure difference between the gas
 260 bubble and its environment, the solubility, the bubble size,
 261 the rise velocity, and adsorbed surfactants [e.g., *Clift et al.*,
 262 1978]. It is unlikely that these parameters are different at
 263 NHR and SHR and thus could explain why the bubble
 264 plumes last about three times longer at SHR. Instead, we
 265 propose that formation of a methane hydrate skin around the
 266 bubbles as they enter the water column explains their
 267 modified behavior throughout the GHSZ, which includes
 268 decreased shrinking rates. This concept was first suggested
 269 by *Maini and Bishnoi* [1981] and has been confirmed in by
 270 other controlled experiments [*Topham*, 1978; *Brewer et al.*,
 271 1998; *Rehder et al.*, 2002]. At natural seeps it was suggested
 272 by *Merewether et al.* [1985].

273 [16] The consistency of the acoustic plume height at
 274 ~ 480 m below the sea surface also supports the idea of
 275 gas hydrate amouring of the rising bubbles, since this water
 276 depth is very close to the upper limit of the GHSZ. Above
 277 Hydrate Ridge, this limit should be at about 505 to 485 m

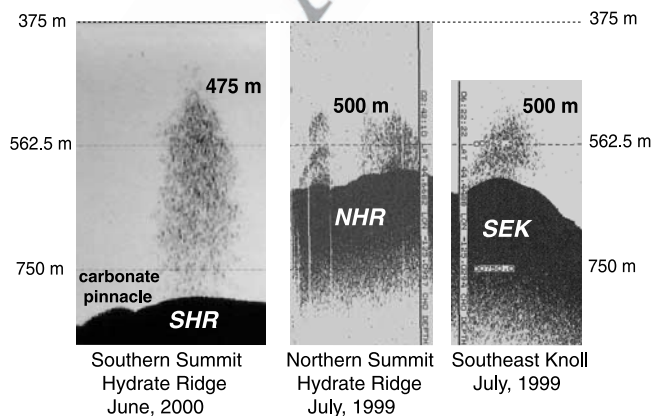


Figure 4. Height of the acoustic signals from the vent sites at SHR, NHR and SEK. The depth above the acoustic signals marks their upper limit. Despite the variable seafloor depth, the acoustic signals at all sites extend to around 480 m.

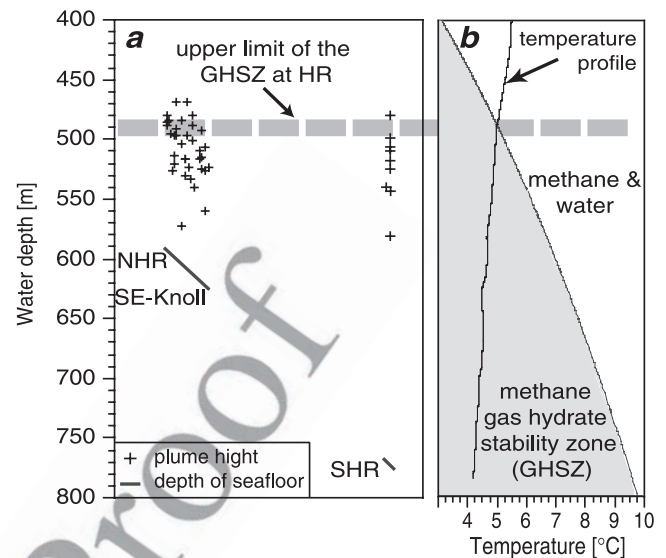


Figure 5. Relationship between the height of the acoustic backscatter images from 12 and 18.5 kHz sources and the upper limit of the gas hydrate stability zone. (a) shows the heights of the acoustic signals at NHR, SEK and SHR (crosses) and the corresponding sea floor depth (bar). In (b) the upper limit of the gas hydrate stability field (gray) at HR is derived from an equation of *Dickens and Quinby-Hunt* [1994] for pure methane gas using the temperature profiles taken at SHR during the cruise AT3-35b [*Torres et al.*, 1999].

278 based on the equation from *Dickens and Quinby-Hunt*
 279 [1994] and various temperature profiles gained on hydrocast
 280 investigations (Figure 5). Therefore the rapid disappearance
 281 of the acoustic signals, which were observed in the back-
 282 scatter data can be interpreted to be the result of the fast
 283 dissolution of the gas hydrate skin and the subsequently
 284 enhanced shrinking of the residual gas bubbles soon after
 285 they rise above the stability zone. It can be argued that due
 286 to the low sensitivity of the acoustic system and the
 287 decreasing target strength caused by the scattering of the
 288 shrinking bubbles, the depth of complete dissolution can not
 289 be resolved. However, the results of the acoustic data are
 290 supported by the depth distribution of the stable carbon
 291 isotopic ratio of methane, $\delta^{13}\text{C}\text{-CH}_4$ vs. Peedee Belemnite
 292 (PDB), in the water column above the vent sites at Hydrate
 293 Ridge [*Heeschen and Collier*, 2002]. Whereas the influence
 294 of the biogenic, isotopically light vent methane with $\delta^{13}\text{C}\text{-}$
 295 CH_4 of $-60 \pm 6\text{‰}$ PDB could be seen within the GHSZ,
 296 this isotopic signature quickly shifted towards -30‰ PDB
 297 at water depths shallower than 480 m. This heavier, ther-
 298 mogenic methane likely originates from sources on the
 299 upper continental slope and appears to dominate over any
 300 methane that might penetrate from below. In only a few
 301 cases did a strong acoustic signal at NHR penetrate above
 302 the GHSZ. These rare acoustic events were also supported
 303 by the presence of $\delta^{13}\text{C}\text{-CH}_4$ signatures lighter than -40‰
 304 PDB in water samples of corresponding depth.

5. Conclusions

[17] This study, which analyzed sites of naturally sourced
 methane plumes that emerge into the ocean within the

308 hydrate stability zone, provides strong supporting evidence
 309 for the importance of the “hydrate skin” mechanism for
 310 influencing the transport of methane through the water
 311 column. It also provides evidence for the stability of these
 312 plumes over time scales of years and underlines the impor-
 313 tance of calibrated, long-term acoustic observatories for
 314 evaluating methane flux from bubbling methane vents on
 315 the seafloor.

316 [18] **Acknowledgments.** We greatly appreciate the support at sea by
 317 the masters and crews of R/V Atlantis, R/V Sonne, R/V Thompson and R/V
 318 Wecoma. We also thank Marta Torres and Magnus Eek for their indispen-
 319 sable help at sea. Financial support for this work was granted by the
 320 National Science Foundation (OCE-9731157; OCE-9811-471, OCE-9731-
 321 23, and OCE-9906990) and the German Federal Ministry of Education and
 322 Research (Fkz 03G0143A and 03G0148A).

323 References

324 Biebow, N., et al., Cruise reports: KOMEX V and VI, *Geomar Rep.* 88, 296
 325 pp., Res. Cent. for Mar. Geosci., Kiel, Germany, 2000.
 326 Bohrmann, G., et al., RV SONNE cruise report SO143, TECFLUX-I-1999,
 327 *Geomar Rep.* 93, 217 pp., Res. Cent. for Mar. Geosci., Kiel, Germany,
 328 1999.
 329 Brewer, P. G., et al., Gas hydrate formation in the deep sea: In-situ experi-
 330 ments with controlled release of methane, natural gas, and carbon diox-
 331 ide, *Energ. Fuels*, 12, 183–188, 1998.
 332 Carson, B., G. K. Westbrook, R. J. Musgrave, and E. Suess (Eds.), *Pro-
 333 ceedings of the Ocean Drilling Program: Scientific Results*, vol. 146,
 334 Ocean Drill. Program, College Station, Tex., 1995.
 335 Clague, D. A., N. Maher, and C. K. Paull, High-resolution multibeam
 336 survey of Hydrate Ridge, offshore Oregon, in *Natural Gas Hydrates: Oc-
 337 currence, Distribution, and Detection*, *Geophys. Monogr. Ser.*, vol. 124,
 338 edited by C. K. Paull and W. P. Dillon, pp. 297–303, AGU, Washington,
 339 D. C., 2001.
 340 Clay, C. S., and H. Medwin, *Acoustical Oceanography*, 537 pp., John
 341 Wiley, New York, 1977.
 342 Clift, R., J. R. Grace, and M. E. Weber, *Bubbles, Drops, and Particles*, 380
 343 pp., Academic, San Diego, Calif., 1978.
 344 Dickens, G. R., and M. S. Quinby-Hunt, Methane hydrate stability in sea-
 345 water, *Geophys. Res. Lett.*, 21(19), 2115–2118, 1994.
 346 Greinert, J., G. Bohrmann, and E. Suess, Gas hydrate-associated carbonates
 347 and methane-venting at Hydrate Ridge: Classification, distribution, and
 348 origin of authigenic lithologies, in *Natural Gas Hydrates: Occurrence,
 349 Distribution, and Detection*, *Geophys. Monogr. Ser.*, vol. 124, edited by
 350 C. K. Paull and W. P. Dillon, pp. 99–113, AGU, Washington, D. C., 2001.
 351 Heeschen, K. U., and R. W. Collier, The flux of methane from hydrates and
 352 seeps to the NE Pacific Ocean off Oregon, *GSA Abstr. Programs*, 34(5),
 353 35,231–XXXXX, 2002.
 354 Linke, P., E. Suess, and Ship's Crew, RV Sonne cruise report SO148,
 355 TECFLUX-II-2000, *Geomar Rep.* 98, 122 pp., Res. Cent. for Mar. Geosci.,
 356 Kiel, Germany, 2001.
 357 MacDonald, I. R., et al., Transfer of hydrocarbons from natural seeps to the
 358 water column and atmosphere, *Geofluid*, 2(2), 95–107, 2002.
 359 MacKay, M. E., et al., Landward vergence and oblique structural trends in
 360 the Oregon margin accretionary prism: Implications and effect on fluid
 361 flow, *Earth Planet. Sci. Lett.*, 109, 477–491, 1992.

Maini, B. B., and P. R. Bishnoi, Experimental investigation of hydrate
 362 formation behavior of a natural gas bubble in a simulated deep sea en-
 363 vironment, *Chem. Eng. Sci.*, 36, 183–189, 1981.
 364 Merewether, R., M. S. Olsson, and P. Lonsdale, Acoustically detected
 365 hydrocarbon plumes rising from 2-km depths in Guaymas Basin, Gulf
 366 of California, *J. Geophys. Res.*, 90(B4), 3075–3085, 1985.
 367 Paull, C. K., W. I. Ussler, W. S. Borowski, and F. N. Spiess, Methane-rich
 368 plumes on the Carolina continental rise: Associations with gas hydrates,
 369 *Geology*, 23(1), 89–92, 1995.
 370 Rehder, G., P. W. Brewer, E. T. Peltzer III, and G. Friederich, Enhanced
 371 lifetime of methane bubble streams within the deep ocean, *Geophys. Res.
 372 Lett.*, 29(15), 1731, doi:10.1029/2001GL013966, 2002.
 373 Salyuk, A., et al., Hydroacoustic flare imaging and estimation of the
 374 methane flux from an active natural methane vent area of the northern
 375 Sakhalin slope, in *Climate Drivers of the North, Program and Abstracts*,
 376 *Terra Nostra*, 2002 (3), pp. 96–97, Alfred-Wegener-Stiftung, Bremerhav-
 377 en, Germany, 2002.
 378 Suess, E., et al., Gas hydrate destabilization: Enhanced dewatering, benthic
 379 material turnover and large methane plumes at the Cascadia convergent
 380 margin, *Earth Planet. Sci. Lett.*, 170, 1–15, 1999.
 381 Suess, E., et al., Sea floor methane hydrates at Hydrate Ridge, Cascadia
 382 margin, in *Natural Gas Hydrates: Occurrence, Distribution, and Detec-
 383 tion*, *Geophys. Monogr. Ser.*, vol. 124, edited by C. K. Paull and W. P.
 384 Dillon, pp. 87–98, AGU, Washington, D. C., 2001.
 385 Topham, D. R., Observations of the formation of hydrocarbon gas hydrates
 386 at depth in seawater, *IOS note 44*, Inst. of Oceans Sci., Sidney, B. C.,
 387 Canada, 1978.
 388 Torres, M. E., et al., Geochemical observations on Hydrate Ridge, Cascadia
 389 margin during R/V-ATLANTIS cruise AT 3-35b, July 1999, *COAS-Data
 390 Rep.174*, 87 pp., Oregon State Univ., Corvallis, Oregon, 1999.
 391 Torres, M. E., et al., Fluid and chemical fluxes in and out of sediments
 392 hosting methane hydrate deposits on Hydrate Ridge, OR: I. Hydrological
 393 provinces, *Earth Planet. Sci. Lett.*, 201, 525–540, 2002.
 394 Tréhu, A. M., and Bangs, 3-D imaging of an active margin hydrate system,
 395 Oregon continental margin, report of cruise TTN112, *COAS-Data
 396 Rep.182*, Oregon State Univ., Corvallis, Oregon, 2001.
 397 Tréhu, A. M., G. Lin, E. Maxwell, and C. Goldfinger, A seismic reflection
 398 profile across the Cascadia subduction zone offshore central Oregon:
 399 New constraints on methane distribution and crustal structure, *J. Geo-
 400 phys. Res.*, 100(B8), 15,101–15,116, 1995.
 401 Tréhu, A. M., et al., Temporal and spatial evolution of a gas hydrate-bearing
 402 ridge on the Oregon continental margin, *Geology*, 27(10), 939–942,
 403 1999.
 404 Tryon, M. D., K. M. Brown, M. E. Torres, A. M. Tréhu, J. McManus, and
 405 R. W. Collier, Measurements of transient and downward fluid flow near
 406 episodic methane gas vents, Hydrate Ridge, Cascadia, *Geology*, 27(12),
 407 1075–1078, 1999.
 408 Tryon, M. D., K. M. Brown, and M. E. Torres, Fluid and chemical flux in
 409 and out of the sediments, hosting methane hydrate deposits on Hydrate
 410 Ridge, OR, II: Hydrological processes, *Earth Planet. Sci. Lett.*, 201,
 411 541–557, 2002.
 412

K. Heeschen, G. Rehder, and E. Suess, Research Center for Marine
 414 Geosciences, Research Center for Marine Geology, D-24148 Kiel, Ger-
 415 many. (kheeschen@geomar.de)
 416 A. Tréhu and R. Collier, College of Oceanographic and Atmospheric
 417 Sciences, Oregon State University, Corvallis, OR 97331-5503, USA.
 418